

## X-Ray Photoelectron Spectroscopy and Catalytic Activity of $\alpha$ -Zirconium Phosphate and Zirconium Phosphate Sulfophenylphosphonate

JORGE L. COLÓN, DEEPAK S. THAKUR, CHAO-YEUEH YANG, ABRAHAM CLEARFIELD,<sup>1</sup>  
AND CHARLES R. MARTIN<sup>1</sup>

*Department of Chemistry, Texas A&M University, College Station, Texas 77843*

Received July 31, 1989; revised January 24, 1990

X-ray photoelectron spectroscopic (XPS) analyses were performed on  $\alpha$ -zirconium phosphate (ZrP) and on an organic derivative of ZrP, zirconium phosphate sulfophenylphosphonate (ZrPS). The XPS results show that the change of half of the phosphate groups in ZrP to sulfophenylphosphonate groups in ZrPS changes the binding energy levels for some electrons in the solid. The XPS analyses also show that upon intercalation of  $\text{Ru}(\text{bpy})_3^{2+}$  into ZrPS, the binding energies of the ruthenium and nitrogen atoms of the metal complex are unperturbed relative to the free complex. ZrP samples show increased catalytic activity for dehydration of cyclohexanol with increased acidity of the sample. However, no correlation between Zr 3d or O 1s binding energies and catalytic activity was found. © 1990 Academic Press, Inc.

### INTRODUCTION

Zirconium phosphates (see Fig. 1) are inorganic ion exchange materials with layered structures (*I*).  $\alpha$ -Zirconium phosphate,  $\text{Zr}(\text{HPO}_4)_2 \cdot \text{H}_2\text{O}$  ( $\alpha$ -ZrP), is the most extensively characterized zirconium phosphate (*I–4*).  $\alpha$ -ZrP is composed of layers of Zr atoms; the metal atoms lie nearly in a plane in a pseudo-hexagonal arrangement. Each Zr atom layer has bridging phosphate groups situated alternatively above and below the Zr atom plane (Fig. 1A). Three oxygen atoms of each phosphate group are bonded to three different zirconium atoms; each zirconium atom is octahedrally coordinated by oxygen atoms. The fourth oxygen atom of the phosphate group bears an exchangeable proton. The solid is composed of stacks of these layers with an interlayer distance of 7.6 Å.

Organic derivatives of  $\alpha$ -ZrP can be formed by replacing a fraction of the phosphate groups with phosphonate groups (*5–7*). These organic substituents are covalently

attached to the phosphate groups of  $\alpha$ -ZrP. These organic substituents increase the interlayer distance by protruding into the interlayer space. Yang and Clearfield have recently prepared a partially substituted phenylsulfonate derivative of  $\alpha$ -ZrP (*8–10*). This organoderivative of  $\alpha$ -ZrP is called zirconium phosphate sulfophenylphosphonate,  $\text{Zr}(\text{HPO}_4)(\text{O}_3\text{P}-\text{C}_6\text{H}_4\text{SO}_3\text{H})$  (ZrPS). ZrPS has an interlayer space of 16.1 Å (Fig. 1B) with a much larger interlayer volume than that of  $\alpha$ -ZrP. Since the strongly hydrophilic  $\text{SO}_3\text{H}$  group promotes swelling, ZrPS forms colloids when exposed to aqueous solutions.

The primary objective of the studies reported here was to investigate the effect of the organo substituent on the electronic charge density of ZrP. X-ray photoelectron spectroscopy (XPS) should in principle be suited for obtaining information on the chemical and physical state of the surface of these materials (*11*). We have used XPS to explore the relationship between organo substitution and electronic charge density. The results of these XPS studies are reported here.

<sup>1</sup> To whom correspondence should be addressed.

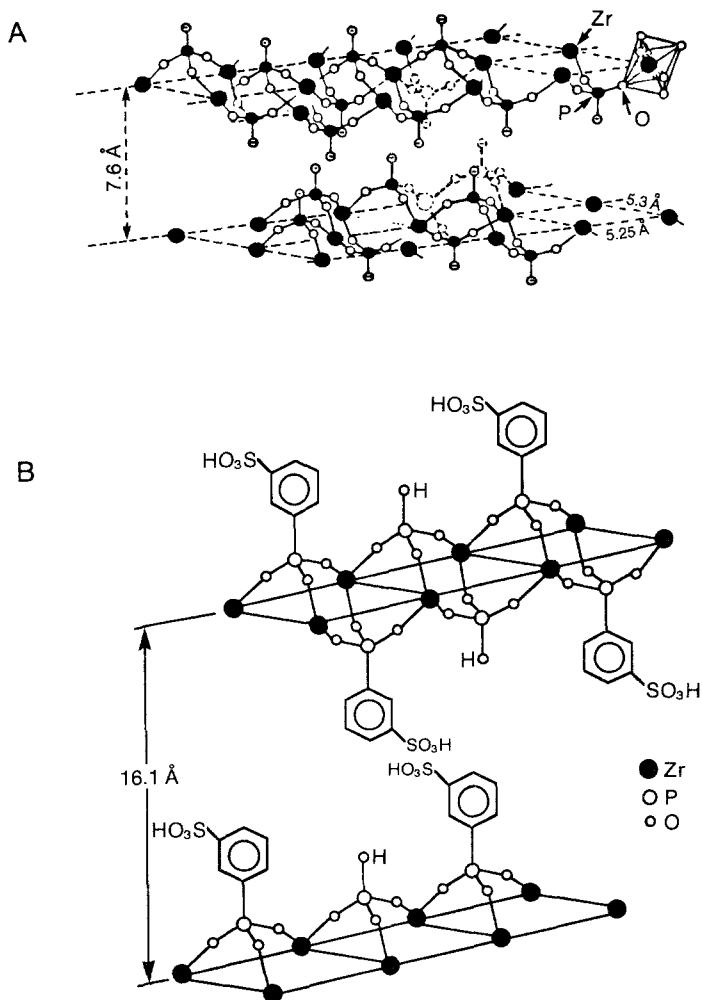


FIG. 1. Idealized structure of (A)  $\alpha$ -ZrP and (B) ZrPS.

In addition to this main objective, the work described here had several secondary objectives. First we have conducted XPS investigations of ZrPS which had been exchanged with the photocatalyst  $\text{Ru}(\text{bpy})_3^{2+}$  (bpy is 2,2'-bipyridine). The objective of these studies was to determine the effect of the chemical microenvironment within ZrPS on the structure and properties of  $\text{Ru}(\text{bpy})_3^{2+}$ . The results of these investigations are also reported here.

Another objective was to evaluate the catalytic activity of zirconium phosphates (12, 13). Zirconium phosphates are acidic

catalysts. The acid-catalyzed decomposition of alcohols has been used as a test reaction for related systems (14–16). In our earlier work (12, 13), we showed that the catalytic activity of zirconium phosphates is related to the number and acidic strength of the hydroxyl groups present on the surface. However, Vinek *et al.* (17) have suggested that the catalytic activity of several phosphates can be related to the oxygen 1s binding energy of the catalysts. We were interested in determining whether this relationship is applicable to ZrP.

The final objective was, therefore, to de-

termine whether XPS can be used to access the catalytic activity of ZrP samples. As part of these catalytic studies, we have conducted XPS investigations on catalytic ZrP samples. These investigations proved that, contrary to the results of Vinek *et al* (17), there is no relationship between the O 1s binding energy and the catalytic activity of the zirconium compounds. In addition, the effect of the crystallinity of the sample on the XPS data was elucidated. The results of these investigations of the catalytic properties of zirconium phosphates are also reported in this paper.

#### EXPERIMENTAL SECTION

**Materials.** Ru(bpy)<sub>3</sub>Cl<sub>2</sub> · 6H<sub>2</sub>O was obtained from G. F. Smith and used as received. Water was either triply distilled or circulated through a Milli-Q water purification system (Millipore Corp.). All other reagents and solvents were of the highest available grade and were used without further purification.

**Procedures.** As noted in the introduction, one of the objectives of this work was to access the effect of crystallinity on the XPS binding energy of the Zr atom. Clearfield *et al.* (18) have shown that the extent of crystallinity in ZrP increases with the concentration of H<sub>3</sub>PO<sub>4</sub> used in the synthesis and with the duration of refluxing during synthesis. Correspondingly, we prepared three batches of ZrP. The first was prepared with 0.5 M H<sub>3</sub>PO<sub>4</sub> and was refluxed for 48 h. These conditions yielded noncrystalline ZrP (labeled here ZrP-0.5:48). The second batch of ZrP was prepared with 4.5 M H<sub>3</sub>PO<sub>4</sub> and was refluxed for 48 h. These conditions yielded semicrystalline ZrP (labeled here ZrP-4.5:48). The final batch was prepared with 12 M H<sub>3</sub>PO<sub>4</sub> and was refluxed for 336 h. These conditions yielded highly crystalline ZrP (ZrP-12:336).

The organic derivative of ZrP (ZrPS is Zr(HPO<sub>4</sub>)(O<sub>3</sub>P-C<sub>6</sub>H<sub>4</sub>SO<sub>3</sub>H), Fig. 1B) was prepared as described previously (8). Ru(bpy)<sub>3</sub><sup>2+</sup> was incorporated (loaded) into ZrPS as described previously (9). ZrPS

samples for XPS analysis were prepared either as KBr pellets or as films on filter paper (9).

**Catalytic activity.** The acid-catalyzed dehydration of cyclohexanol was used to test the catalytic activity of the ZrP samples. This reaction yields cyclohexene and water as the major products and cyclohexanone as a minor product. The amount of cyclohexanone was less than 0.5% for all the ZrP samples.

The catalytic activity for cyclohexanol dehydration was determined at 400°C in a continuous flow reactor pretreated as described elsewhere (12, 13). The flow of the reactants was metered with a Sage syringe pump. Products were analyzed on a gas chromatography column packed with 10% OV-17 on 100/120 Chromosorb WHP. The quantity of cyclohexanol converted to cyclohexene was monitored as a function of contact time in the reactor; these data were analyzed via a pseudo-first-order rate expression. The catalytic activity is given as the first-order rate constant.

**Instrumentation.** X-ray photoelectron spectroscopy (XPS) analyses of the ZrPS samples were performed at the Surface Science Facility at Texas A&M University by using a Kratos XSAM-800 spectrometer. Primary excitation was provided by a Mg anode biased at 12 kV with 20 mA of filament current. The spectra were collected by using a fixed analyzer transmission mode on a hemispherical electron analyzer. The binding energies for the spectra were referenced to the C 1s line, which was fixed at 285 eV.

For the catalytic experiments, XPS analyses of the zirconium compounds were performed on a Hewlett-Packard 5950-A ESCA spectrometer. The excitation radiation was AlK $\alpha$  ( $h\lambda = 1486.6$  eV). The sample was gently ground under dry nitrogen inside a glovebox and mounted onto the sample holder. The sample was allowed to outgas for 1 h in the sample preparation chamber before introduction into the spectrometer. An electron flood gun was used to

control charging effects. Sufficient scanning was used to obtain peak heights of at least 5 K counts over the background; peak heights of 10–20 K counts were normally used. The decomposition of the peaks was performed using the XPS spectrometer's nonlinear least-squares decomposition software. The C 1s line at 285 eV was used as reference.

#### RESULTS AND DISCUSSION

*Comparison of zirconium and phosphorus XPS data for ZrP and ZrPS.* Figure 2 shows typical XPS spectra for free  $\text{Ru}(\text{bpy})_3^{2+}$ , unexchanged ZrPS, and  $\text{Ru}(\text{bpy})_3^{2+}$ -exchanged ZrPS. Tables 1, 2, and 3 show the core level binding energy values for different elements in the ZrPS and  $\alpha$ -ZrP samples. The following discussion will explain the results for the different elements and compare these results to other reported XPS experiments with zirconium phosphates. First, the Zr 3d binding energies of ZrPS will be compared with the corresponding binding energies for ZrP obtained from the literature (19, 20) and from the present investigations. The objective of these comparisons is to elucidate the effect, if any, of the  $-\text{C}_6\text{H}_4\text{SO}_3\text{H}$  substituent on the binding energy values of ZrPS.

Figure 3 shows the Zr  $3d_{3/2}$  and Zr  $3d_{5/2}$  region of the XPS spectra of ZrPS and Table 1 lists the binding energy data obtained from the peaks in Fig. 3. The separation between the two Zr 3d peaks in ZrPS is 2.3–2.4 eV. This peak separation is in good agreement with the Zr 3d peak separation in ZrP (2.2–2.3 eV (19), 2.3–2.5 eV (20), and 2.3–2.6 eV, this work) and is characteristic of Zr(IV) compounds. This confirms that the ZrPS synthesis has yielded the layered acid phosphate of tetravalent zirconium (8); i.e., that the incorporation of the  $-\text{C}_6\text{H}_4\text{SO}_3\text{H}$  group does not change the valence state of the zirconium atoms.

Figure 4 shows the XPS spectra of the Zr 3d region for the various ZrP samples and for the other zirconium compounds investigated in this study; Table 2 presents the

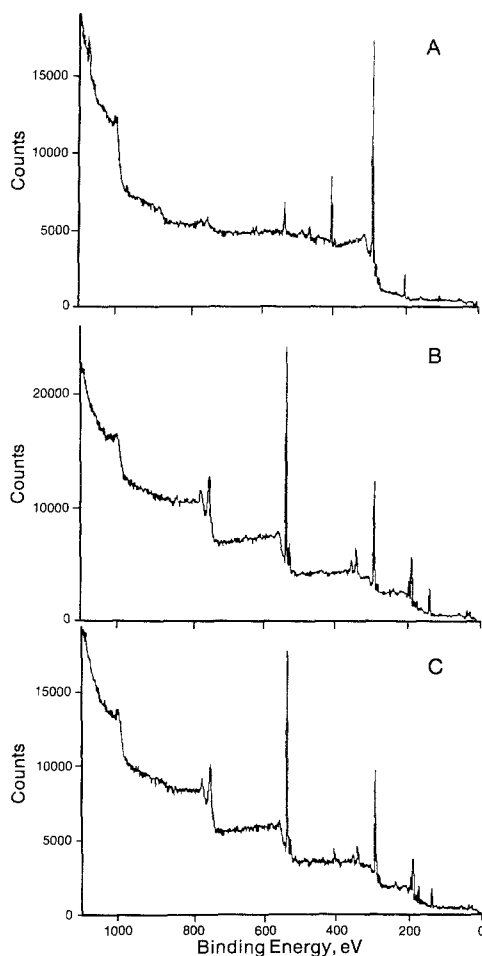


FIG. 2. X-ray photoelectron spectra of (A)  $\text{Ru}(\text{bpy})_3\text{Cl}_2$ , (B) ZrPS, and (C)  $\text{Ru}(\text{bpy})_3^{2+}$ -exchanged ZrPS.

binding energy data obtained from these spectra. The Zr  $3d_{5/2}$  binding energies for  $\text{ZrO}_2$ ,  $\text{Zr}(\text{SO}_4)_2$ , ZrP-0.5:48 (noncrystalline), and ZrP-12:36 (highly crystalline) are identical (184.2 eV) (Table 2); the binding energy for ZrP-4.5:48 (semicrystalline) is 0.8 eV higher. The same relationship is observed for the Zr  $3d_{3/2}$  binding energies (186.6–186.8 eV for  $\text{ZrO}_2$ ,  $\text{Zr}(\text{SO}_4)_2$ , ZrP-0.5:48, and ZrP-12:36; 187.5 eV for ZrP-4.5:48).

A comparison of the data in Tables 1 and 2 shows that the Zr 3d binding energies of ZrP (Table 2) are higher than the Zr 3d bind-

TABLE 1

Zirconium, Phosphorus, Oxygen, and Sulfur Binding Energies for ZrPS and Ru(bpy)<sub>3</sub><sup>2+</sup>-Exchanged ZrPS

Binding energies <sup>a,b</sup> (eV)						
Ru(bpy) <sub>3</sub> <sup>2+</sup> (%) <sup>c</sup>	Zr 3d <sub>3/2</sub>	Zr 3d <sub>5/2</sub>	P 2s	P 2p <sub>3/2</sub>	O 1s	S 2p <sub>3/2</sub>
0	186.1	183.7	191.5	134.1	532.0	169.0
					533.7	
1.74	185.9	183.5	191.3	134.1	531.9	—
					533.5	
4.34	185.9	183.5	191.4	133.9	531.7	168.9
					533.5	
6.52	185.8	183.4	191.1	134.0	531.8	168.9
					533.4	
13.04	186.0	183.6	191.3	133.9	532.0	168.8
					533.5	
15.20	185.8	183.5	191.2	—	531.6	—
					532.9	
21.75	186.0	183.6	191.2	133.9	531.8	168.7
					533.4	

<sup>a</sup> The binding energies are referenced to the C 1s line, which was fixed at 285 eV.

<sup>b</sup> For electrons with two BE values the decomposition of the corresponding peaks was performed with a nonlinear least-squares program of the spectrometer software (Autofit command in Peak Synthesis).

<sup>c</sup> Percent of  $-\text{SO}_3^-$  sites in ZrPS occupied by Ru(bpy)<sub>3</sub><sup>2+</sup>.

ing energies for ZrPS (Table 1). The reduced Zr 3d binding energies observed for the ZrPS samples indicate a reduced polarization of the Zr–O bonds in ZrPS (19). We can minimize the effect of charging in the binding energy comparison by considering not only absolute, but also relative chemical shifts. The difference in photoelectron

TABLE 2

Zirconium 3d, Oxygen 1s, and Phosphorus 2s Binding Energies for Various Catalytic Zirconium Compounds

Binding energies (eV)				
Compound	Zr 3d <sub>3/2</sub>	Zr 3d <sub>5/2</sub>	O 1s	P 2s
ZrO <sub>2</sub> (monoclinic)	186.8	184.2	530.9	—
Zr(SO <sub>4</sub> ) <sub>2</sub> (anhyd)	186.6	184.2	532.0	—
$\alpha$ -ZrP(0.5:48)	186.6	184.2	532.9	192.0
$\alpha$ -ZrP(4.5:48)	187.5	185.0	533.3	192.8
$\alpha$ -ZrP(12:336)	186.6	184.2	533.0	192.0
$\alpha$ -ZrP <sup>a</sup> (hydrated)	187.8	185.5	533.3	193.4
$\alpha$ -ZrP <sup>a</sup> (dehydrated)	188.1	185.9	533.4	193.8
$\gamma$ -ZrP <sup>a</sup> (hydrated)	187.3	185.0	532.7	193.0

<sup>a</sup> Ref. (19).

TABLE 3

Ruthenium 3d and Nitrogen 1s Binding Energies for Ru(bpy)<sub>3</sub><sup>2+</sup>-Exchanged ZrPS

Binding energies <sup>a,b</sup> (eV)		
Ru(bpy) <sub>3</sub> <sup>2+</sup> (%) <sup>c</sup>	Ru 3d <sub>5/2</sub>	N 1s
Ru(bpy) <sub>3</sub> Cl <sub>2</sub>	280.8	399.9
0	—	402.1
1.74	281.2	399.8
		402.2
4.34	—	—
		401.1
6.52	281.1	400.4
		402.1
13.04	281.0	400.2
		402.0
15.20	281.0	400.2
		402.2
21.75	280.9	400.2
		402.1

<sup>a</sup> The binding energies are referenced to the C 1s line, which was fixed at 285 eV.

<sup>b</sup> For electrons with two BE values the decomposition of the corresponding peaks was performed with a nonlinear least-squares program of the spectrometer software (Autofit command in Peak Synthesis).

<sup>c</sup> Percentage of  $-\text{SO}_3^-$  sites in ZrPS occupied by Ru(bpy)<sub>3</sub><sup>2+</sup>.

energies between two electrons in two different samples gives useful chemical shift information since charging effects cancel out in an energy difference. The Zr 3d<sub>5/2</sub>–O 1s binding energy difference in  $\alpha$ -ZrP is 347.5 eV whereas in ZrPS the difference is 348.3 eV. This observation also suggests a reduced polarization of the Zr–O bond in ZrPS (19). ZrPS differs from ZrP in that half of the  $-\text{OH}$  groups in ZrP are replaced by  $-\text{C}_6\text{H}_4\text{SO}_3\text{H}$  groups in ZrPS. Thus, substitution of  $-\text{OH}$  by  $-\text{C}_6\text{H}_4\text{SO}_3\text{H}$  reduces the polarization of the Zr–O bond. This conclusion is corroborated by the phosphorus binding energy data (vide infra).

The phosphorus 2s and 2p<sub>3/2</sub> binding energies for ZrP (Table 2) are higher than the corresponding binding energies for ZrPS (Table 1). Alberti *et al.* (19) compared the P 2s binding energy of ZrP to the P 2s bind-

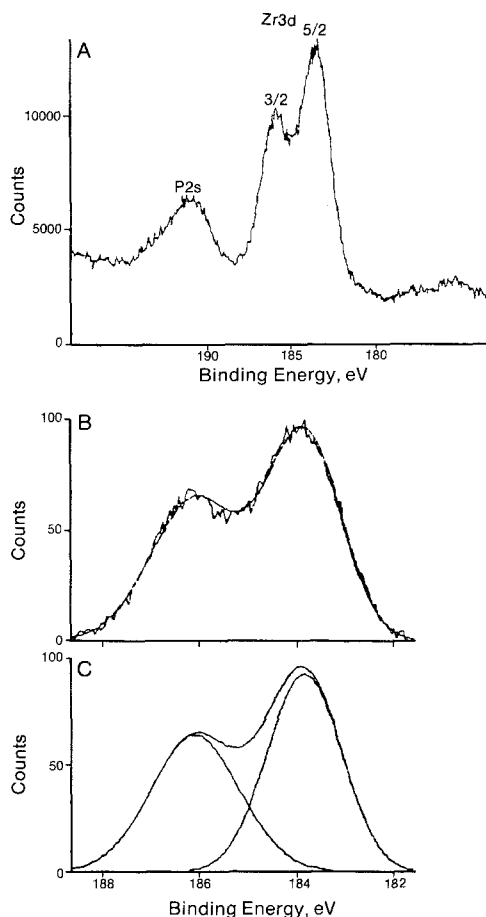


FIG. 3. X-ray photoelectron spectra of (A) ZrPS P  $2s$ , Zr  $3d_{3/2}$ , and Zr  $3d_{5/2}$  binding energy region; (B) least-squares fit to Zr  $3d$  binding energy region; and (C) Zr  $3d$  peak decomposition.

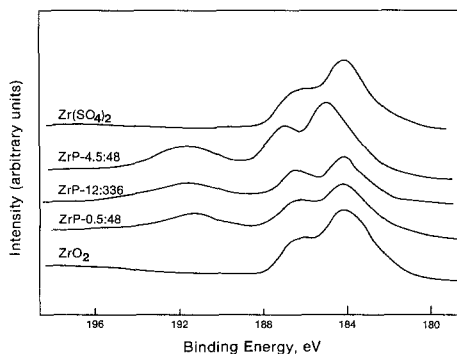


FIG. 4. Zirconium  $3d$  binding energy region of the XPS spectra of  $\alpha$ -ZrP samples,  $Zr(SO_4)_2$ , and  $ZrO_2$ .

ing energies for Fe, Al, and Ga phosphates; again, the ZrP binding energies were found to be higher. Alberti *et al.* (19) attributed the higher P  $2s$  binding energy in ZrP to the increased polarity of the O–P bond in this compound. The O–P bond polarity is enhanced due to polarization induced by the proton bonded to the phosphorus atoms in ZrP.

The above analysis suggests that the reduced phosphorus binding energies for ZrPS relative to ZrP (Tables 1 and 2) are attributable to the diminution in O–P polarization associated with the replacement of –OH groups with  $-C_6H_4SO_3H$  groups. The identical conclusion was reached through an analysis of the Zr  $3d$  binding energy data (*vide supra*). Again, to rule out any charging effects, we should compare binding energy differences. Alberti *et al.* (19) have suggested that the binding energy difference between P  $2s$  (or P  $2p$ ) and O  $1s$  should be used when comparing binding energy values between phosphate-containing compounds.

The average P  $2s$ –O  $1s$  difference for ZrPS is 340.6 eV (Table 1); Alberti *et al.* (19) found a P  $2s$ –O  $1s$  difference of 340 eV for ZrP and a difference of 341.5 eV for Fe, Al, and Ga phosphates. A smaller P  $2s$ –O  $1s$  difference corresponds to a higher extent of polarization of the P–O bond. The ZrPS value is intermediate between that of ZrP and the trivalent phosphates, indicating an intermediate P–O polarization caused by the existence of both P–OH and P– $C_6H_4SO_3H$  groups in ZrPS.

*Comparison of oxygen XPS data for ZrP and ZrPS.* The Zr and P XPS data suggest that the Zr–O and P–O bonds are more polarized in ZrP than in ZrPS. What can the O  $1s$  XPS data from these compounds tell us about the charge distribution and chemical characteristics of these systems? Figure 5 shows that the O  $1s$  band for ZrPS is structured. The main peak is centered at 532.0 eV (Table 1); a shoulder (centered at 533.7 eV) occurs on the high binding energy side of the main peak. The main peak is attrib-

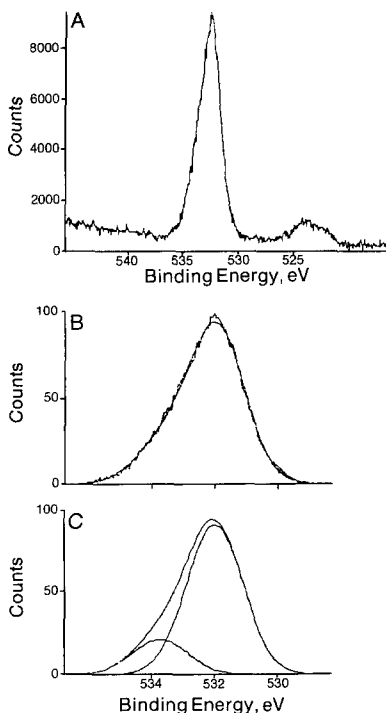


FIG. 5. (A) X-ray photoelectron spectra of ZrPS O 1s binding energy region; (B) least-squares fit to O 1s binding energy region; and (C) O 1s peak decomposition.

uted to the oxygens of the phosphate and sulfonate groups (19–21) (the sulfur 2p binding energy was also observed in these samples). The shoulder is due to the –OHs bonded to phosphorus.

In contrast to the ZrPS samples, the O 1s peak in ZrP must be resolved into three component peaks (Fig. 6). The main peak is centered around 533 eV with a shoulder at higher binding energy and a smaller shoulder at lower binding energy. Alberti *et al.* (19) also found that the O 1s peak of ZrP could be resolved into three component peaks. Alberti *et al.* (19) attributed the low energy shoulder to surface Zr–OH groups formed through hydrolytic reactions. This is corroborated by the fact that Zr(OH)<sub>4</sub> shows a O 1s binding energy at lower energies than the zirconium phosphates (19). Since the ZrPS samples do not show the lower binding energy shoulder on the O 1s

band, hydrolytic reactions are not occurring in ZrPS. This conclusion is corroborated by the fact that IR spectra for ZrPS (8) do not show a vibrational peak characteristic of a Zr–OH group.

The binding energy of the O 1s main peak in ZrPS is smaller than the O 1s energy in ZrP (Fig. 6 and Table 2). This reduction in O 1s binding energy for ZrPS is again attributed to the replacement of –OH with –C<sub>6</sub>H<sub>4</sub>SO<sub>3</sub>H in half of the phosphate groups in ZrPS. However, we have pointed out above that the differences in Zr 3d and P 2s binding energies between ZrP and ZrPS are attributed to a higher Zr–O and P–O bond polarization in the ZrP samples. This interpretation suggests that the electronic charge density surrounding the oxygen atom should be greater in ZrP than that in ZrPS. If this is true then we should have observed a O 1s binding energy for ZrP lower (due to charge transfer) than that for ZrPS; the opposite was observed. This apparent contradiction can be explained by taking into consideration the structure of ZrP and ZrPS.

A lower O 1s binding energy in ZrP than in ZrPS is not observed because the charge transfer occurs over all the oxygens coordinated to the zirconium and the phosphorus. There are six oxygen atoms coordinated to every Zr atom in ZrP. Therefore, the effect

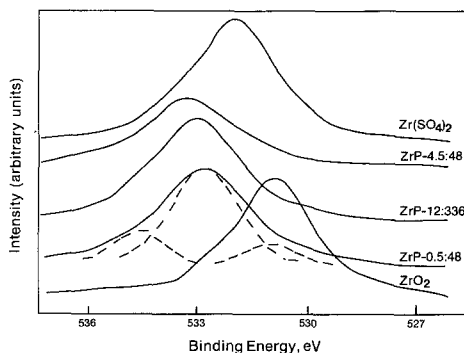


FIG. 6. Oxygen 1s region of the XPS spectra of  $\alpha$ -ZrP samples, Zr(SO<sub>4</sub>)<sub>2</sub>, and ZrO<sub>2</sub>. Dashed curve shows decomposition of the O 1s peak for the ZrP 0.5:48 sample.

of any change in polarization will be felt entirely by the Zr atom whereas each of the oxygens coordinated to this Zr atom will only feel a partial change. The charge density change felt by each oxygen can be small enough as to be undetectable. This is why Alberti *et al.* did not observe any binding energy shift for O 1s of ZrP relative to other phosphate compounds (19).

This polarization effect observed in ZrP (due to the relative number of Zr, P, and O atoms) should also be observed in ZrPS. However, in ZrPS only three oxygens are in the same coordination environment as the oxygens coordinated to Zr in ZrP. The three other oxygens in ZrPS are bonded to a phosphorus having a sulfophenylphosphonate substituent; this substituent is not present in ZrP. In addition, ZrPS has three oxygens as part of the sulfonate group in the sulfophenylphosphonate substituent. The binding energy of an O 1s in a sulfonate group is about 532 eV (Ref. (21) and Table 2) which is exactly the O 1s binding energy observed in our ZrPS samples. The different environment for oxygen in ZrPS compared to that in ZrP suggests that the lower O 1s binding energy observed in ZrPS comes from the oxygens in the sulfonate group. The change in electronic charge density for the oxygens coordinated to Zr in ZrP is not big enough to shift its binding energy to lower values than those in ZrPS.

It is important to point out that final state relaxation (22) can be ruled out as a contributor to these binding energy shifts. Final state relaxation would have affected these two related compounds (ZrP and ZrPS) to a similar extent. In addition, final state relaxation occurs to a lesser extent in insulators than in metals (22). Therefore, our data indicate that the difference in Zr–O and P–O bond polarization is the reason for the chemical shifts observed in the binding energies.

*XPS studies of Ru(bpy)<sub>3</sub><sup>2+</sup>-exchanged ZrPS.* The objective of the XPS studies of Ru(bpy)<sub>3</sub><sup>2+</sup>-exchanged ZrPS was to elucidate the effect (if any) of the interlayer

microenvironment on the intercalated Ru(bpy)<sub>3</sub><sup>2+</sup> counterion. We have previously reported the XPS spectra of Ru(bpy)<sub>3</sub>Cl<sub>2</sub> and of Ru(bpy)<sub>3</sub><sup>2+</sup> exchanged into ZrPS samples (6.52% of the sulfonate sites were exchanged with Ru(bpy)<sub>3</sub><sup>2+</sup>) (6). We present in Tables 1 and 3 binding energies for ZrPS samples containing a broad range of concentrations of Ru(bpy)<sub>3</sub><sup>2+</sup>. All binding energy values were found to be independent of concentration of Ru(bpy)<sub>3</sub><sup>2+</sup> in ZrPS.

The binding energy for Ru 3d<sub>5/2</sub> in Ru(bpy)<sub>3</sub>Cl<sub>2</sub> is at 280.8 eV; the binding energy for Ru 3d<sub>5/2</sub> in Ru(bpy)<sub>3</sub><sup>2+</sup> which has been incorporated into ZrPS is 280.9–281.2 eV. These values are in accord with literature values for Ru(bpy)<sub>3</sub><sup>2+</sup> and other Ru(II) compounds (23–30). The binding energy for a Ru(III) ion would be 2.3 eV more positive than that for a Ru(II) ion (26, 31). Since our binding energy values are similar to those for other Ru(II) species, we can rule out any electronic modification (i.e., partial oxidation) of Ru(bpy)<sub>3</sub><sup>2+</sup> upon intercalation. In addition, the Zr 3d binding energy values observed when Ru(bpy)<sub>3</sub><sup>2+</sup> is exchanged into ZrPS do not differ from the values for ZrPS which is devoid of Ru(bpy)<sub>3</sub><sup>2+</sup>. Thus, the introduction of the metal complex into the interlayer space of ZrPS does not influence the electronic charge density of the zirconium atoms.

Table 3 indicates that the ZrPS which is devoid of Ru(bpy)<sub>3</sub><sup>2+</sup> shows a N 1s XPS signal. This N 1s signal arises from some unidentified impurity in ZrPS. This impurity is also present in the Ru(bpy)<sub>3</sub><sup>2+</sup>-exchanged ZrPS samples (Table 3). The alternate explanation for the presence of the 402.1 eV peak in the Ru(bpy)<sub>3</sub><sup>2+</sup>-exchanged samples is that protonation of a bpy ligand occurs within the interlayer space of ZrPS (20, 32, 33). We have previously reported results of careful infrared and UV-visible spectroscopic investigations of Ru(bpy)<sub>3</sub><sup>2+</sup>-exchanged ZrPS (9). The intent of these investigations was to determine if evidence for protonation of a bpy ligand could be gathered. We found no evidence for protonation



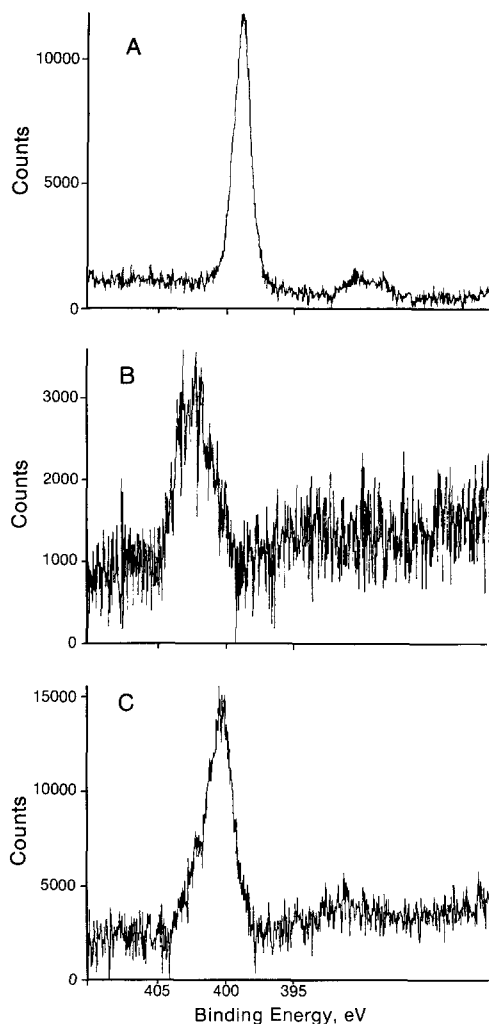


FIG. 7. X-ray photoelectron spectra showing the N 1s binding energy region of (A)  $\text{Ru}(\text{bpy})_3\text{Cl}_2$ , (B) ZrPS, and (C)  $\text{Ru}(\text{bpy})_3^{2+}$ -exchanged ZrPS.

of the bpy's in  $\text{Ru}(\text{bpy})_3^{2+}$ -exchanged ZrPS (9). Hence, the 402.1 XPS peak observed in these samples is due to an impurity (Fig. 7).

**Catalytic studies.** In recent years, it has been recognized that dehydration of alcohol requires both electron donor and electron acceptor sites (14–16). The strength of acidic and basic sites determines the catalytic activity and selectivity. Vinek *et al.* (17) and Noller and Kladning (34) have proposed that the XPS binding energy values for cationic and anionic sites can be used as

a measure of acidity/basicity or electron pair accepting/donating (EPA or EPD) capability of a given catalytic compound. The increase in binding energy for a cationic site indicates an increase in its EPA strength, while the increase in binding energy for an anionic site indicates lower EPD strength.

Using a series of magnesium compounds as catalysts, Vinek *et al.* (17) have shown that magnesium phosphate, with higher magnesium 2p and oxygen 1s binding energy values, exhibits higher alcohol dehydration activity than other magnesium compounds with lower binding energy values. However, Davis *et al.* (35) found no correlation between the alcohol dehydration activity of several metal oxide catalysts and O 1s binding energy. We have performed cyclohexanol dehydration activity and XPS measurements on a series of catalytic ZrP samples. The idea was to determine whether there exists a correlation between the O 1s binding energy of the ZrP samples and the catalytic activity, as suggested by Vinek *et al.* (17). This study should indicate whether XPS data from ZrP samples can be used to access the catalytic activity of ZrP compounds.

The conversion of cyclohexanol to cyclohexene at 400°C as a function of time was measured for each of the catalysts. Figure 8 presents first-order plots of the cyclohexanol dehydration activity data for the vari-

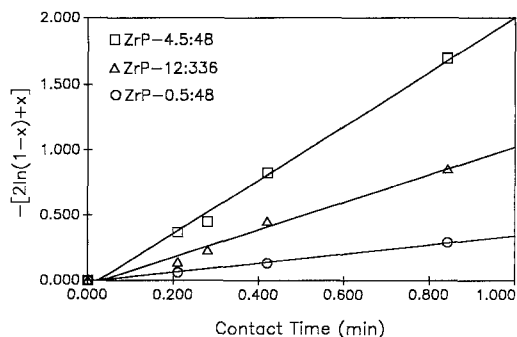


FIG. 8. First-order plots of the cyclohexanol dehydration activity of ZrP samples of varying crystallinity at 400°C.

ous zirconium compounds. The first-order rate constants for cyclohexanol dehydration for the various catalysts were evaluated using the kinetic expression (12, 13)

$$-[2 \ln(1 - x) + x] = kt, \quad (1)$$

where  $x$  is the fractional conversion,  $k$  is the first-order rate constant, and  $t$  is the contact time in minutes, given by the ratio of the weight of the catalyst (g) to the flow rate (g/min). The slopes of the straight lines in Fig. 8 yield the values of the specific reaction rate constants  $k$  ( $\text{min}^{-1}$ ). Dehydrogenation to cyclohexanone was less than 0.5 wt% for the zirconium samples. These results indicate that these phosphates are selective toward cyclohexene formation.

The dehydration activity data in Fig. 8 shows the following trend: ZrP-4.5:48 (semicrystalline) > ZrP-12:336 (highly crystalline) > ZrP-0.5:48 (noncrystalline). However, the activity relationship can be expressed on a per surface area basis by dividing the rate constant by the surface area—ZrP-4.5:48 ( $34.6 \text{ m}^2/\text{g}$ ), ZrP-12:336 ( $1.8 \text{ m}^2/\text{g}$ ), and ZrP-0.5:48 ( $2.7 \text{ m}^2/\text{g}$ ). On a per surface area basis the activities are

$$\begin{array}{rcl} \text{ZrP-12:336} & > & \text{ZrP-0.5:48} \\ (0.50 \text{ g min}^{-1} \text{ m}^{-2}) & & (0.14 \text{ g min}^{-1} \text{ m}^{-2}) \\ & > & \text{ZrP-4.5:48} \\ & & (0.082 \text{ g min}^{-1} \text{ m}^{-2}) \end{array}$$

Therefore, ZrP-12:336 has the highest activity per unit surface area.

An attempt was made to correlate the Zr  $3d_{5/2}$  and O  $1s$  binding energies for various samples with their catalytic activity. Figure 9 shows plots of rate constant vs XPS binding energy. Although ZrP-0.5:48 (noncrystalline) and ZrP-12:336 (highly crystalline) have the same Zr  $3d$  binding energy (Table 2), ZrP-12:336 is three times more active than ZrP-0.5:48 (Fig. 9A). In addition, ZrP-4.5:48 has the highest Zr  $3d$  binding energy, but the smallest activity. Similarly, the three phosphate samples have comparable O  $1s$  binding energies, but their catalytic

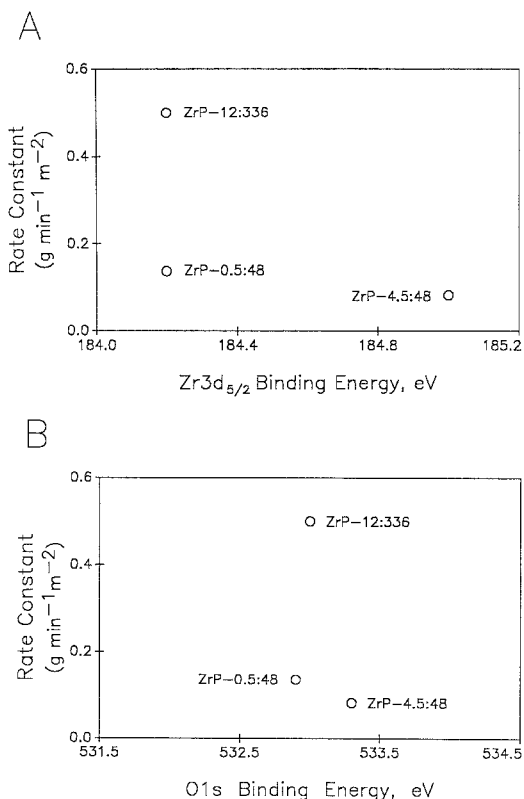


FIG. 9. Variation of dehydration rate constant with (A) Zr  $3d$  binding energy and (B) O  $1s$  binding energy for ZrP samples.

activities differ markedly (Fig. 9B). These results indicate that, contrary to the results of Vinek *et al.*, no correlation exists between binding energy and catalytic activity.

On the basis of these results no clear correlation between catalytic activity and XPS binding energy can be established. Similar conclusions were reached by Davis *et al.* (35) in their catalytic activity investigations by XPS O  $1s$  binding energy studies. These results are reasonable since only one out of four oxygens in the phosphate group bears a proton and XPS analyzes only about  $30 \text{ \AA}$  into the bulk of the material. Therefore, the oxygens present in these surface  $-\text{OH}$  groups do not change the overall binding energy of the main oxygen  $1s$  signal. In fact, the phosphate samples with differing acidities have almost identical O  $1s$  binding

energy. In conclusion, XPS cannot be used to access the catalytic activity of these phosphate samples.

Our previous measurements indicate that catalytic activity for cyclohexanol dehydration depends upon the number and strength of acid sites on the catalyst surface at 400°C (12, 13). For example, ZrP-0.5:48 (noncrystalline) loses most of its surface hydroxyl groups due to excessive dehydroxylation at this temperature, whereas ZrP-4.5:48 (semicrystalline) and ZrP-12:336 (highly crystalline) exhibit maxima at 400°C in the acid strength versus calcination temperature curve. The difference in their catalytic activity should, then, be related to the surface hydroxyl groups (12).

#### CONCLUSIONS

This study has demonstrated that XPS can give some information about the chemical environment in layered zirconium phosphate and its organic derivatives. The comparison made between the XPS binding energies observed in the ZrPS samples and in the ZrP samples have shown that ZrPS and ZrP have similar electronic properties. The binding energy differences between ZrP and ZrPS result from the influence of  $-C_6H_4SO_3H$  groups in ZrPS (absent in ZrP) on the polarization of the bonds in the material. The environment in ZrPS also does not promote any hydrolytic reactions of the Zr atoms.

The environment in ZrPS has no effect on the nature of the intercalated  $Ru(bpy)_3^{2+}$  complex. The binding energies for Ru(II) and bipyridine nitrogen are not affected upon intercalation. No evidence for protonation of the bpy's in  $Ru(bpy)_3^{2+}$ -exchanged ZrPS is observed. In addition, the binding energies in  $Ru(bpy)_3^{2+}$ -exchanged ZrPS are independent of concentration of  $Ru(bpy)_3^{2+}$  in ZrPS.

No correlation between XPS O 1s binding energy and catalytic activity was observed for ZrP. Recently, La Ginestra *et al.* (36) reported catalytic activity measurements for the dehydration of isopropanol

and 1- and 2-butanol, and the isomerization of 1-butene in  $\alpha$ -ZrP. In accord with our conclusions (12, 13), these authors suggest that the active centers in  $\alpha$ -ZrP are the Brønsted sites on the surface. The interlayer region is not involved in the catalytic activity of these materials. The strength of the acidic sites increases upon heating above 350°C. This transformation probably occurs through partial or total transformation of hydrogen phosphate to P-O-P groups with progressive formation of a layered pyrophosphate phase (36, 37).

A small amount of activity is due to a second site (12, 13, 36) which is responsible for the residual catalytic activity observed in the alcohol dehydration on  $Cs^+$ -ZrP. La Ginestra *et al.* (36) have suggested that this residual catalytic activity can be due to new Brønsted sites generated either from the crumbling of the crystallites after interaction with water or from some  $Cs^+$  diffusion into the exchanger and consequent migration of  $H^+$  on the surface. Clearfield and Thakur (12) have suggested that the residual catalytic activity comes from some Lewis sites, associated with the zirconium atoms or with defects caused by hydrolysis of  $HPO_4^{2-}$  groups, which are not poisonable by  $Cs^+$  ions.

#### ACKNOWLEDGMENTS

Financial support for this work was provided by the Robert A. Welch Foundation, the Office of Naval Research, and the Air Force Office of Scientific Research. J.L.C. acknowledges the support from the Texas A&M University Minority Merit Fellowship.

#### REFERENCES

1. Clearfield, A., in "Inorganic Ion Exchange Materials" (A. Clearfield, Ed.). CRC Press, Boca Raton, FL, 1982.
2. Alberti, G., *Acc. Chem. Res.* **11**, 163 (1978).
3. Clearfield, A., and Thakur, D. S., *Appl. Catal.* **26**, 1 (1986).
4. Clearfield, A., *Chem. Rev.* **88**, 125 (1988).
5. Alberti, G., Constantino, U., Allulli, S., and Tomassini, N., *J. Inorg. Nucl. Chem.* **40**, 1113 (1978).
6. Dines, M. B., and DiGiacomo, P. M., *Inorg. Chem.* **20**, 92 (1981).
7. Alberti, G., in "Recent Developments in Ion Ex-

- change" (P. A. Williams, and M. J. Hudson, Eds.), pp. 233-248. Elsevier Applied Science, London, 1987.
8. Yang, C.-Y., and Clearfield, A., *React. Polym. Ion Exch. Sorbents* **5**, 13 (1987).
  9. Colón, J. L., Yang, C.-Y., Clearfield, A., and Martin, C. R., *J. Phys. Chem.* **92**, 5777 (1988).
  10. Colón, J. L., Yang, C.-Y., Clearfield, A., and Martin, C. R., *J. Phys. Chem.* **94**, 874 (1990).
  11. Delgass, W. N., Haller, G. L., Kellerman, R., and Lunsford, J. H., "Spectroscopy in Heterogeneous Catalysis," Chap. 8. Academic Press, New York, 1979.
  12. Clearfield, A., and Thakur, D. S., *J. Catal.* **65**, 185 (1980).
  13. Thakur, D. S., and Clearfield, A., *J. Catal.* **69**, 230 (1981).
  14. Winfield, M. E., in "Catalysis" (P. H. Emmett, Ed.), Vol. VII, p. 93. Reinhold, New York, 1960.
  15. Pines, H., and Manassen, J., in "Advances in Catalysis" (D. D. Eley, H. Pines, and P. B. Weisz, Eds.), Vol. 16, p. 46. Academic Press, San Diego, 1966.
  16. Kibby, C. L., Lande, S. S., and Hall, W. K., *J. Amer. Chem. Soc.* **94**, 214 (1972).
  17. Vinek, H., Noller, H., Ebel, M., and Schwarz, K., *J. Chem. Soc. Faraday Trans. 1* **73**, 734 (1977).
  18. Clearfield, A., Oskarsson, A., and Oskarsson, C., *Ion Exch. Membr.* **1**, 91 (1972).
  19. Alberti, G., Constantino, U., Marletta, G., Puglisi, O., and Pignataro, S., *J. Inorg. Nucl. Chem.* **43**, 3329 (1981).
  20. Mattogno, G., Ferragina, C., Massucci, M., Patrono, P., and La Ginestra, A., *J. Electron Spectrosc. Relat. Phenom.* **46**, 285 (1988).
  21. Lindberg, B. J., Hamrin, K., Johansson, G., Gelius, U., Fahlman, A., Nordling, C., and Siegbahn, K., *Phys. Scr.* **1**, 286 (1970).
  22. Briggs, D., and Seah, M. P. "Practical Surface Analysis." Wiley, London, 1989.
  23. De Wilde, W., Peeters, G., and Lunsford, J. H., *J. Phys. Chem.* **84**, 2306 (1980).
  24. Abdo, S., Canesson, P., Cruz, M., Fripiat, J. J., and Van Damme, H., *J. Phys. Chem.* **85**, 797 (1981).
  25. Weaver, T. R., Meyer, T. J., Adeyemi, S. A., Brown, G. M., Eckberg, R. P., Hatfield, W. E., Johnson, E. C., Murray, R. W., and Untereker, D., *J. Amer. Chem. Soc.* **97**, 3039 (1975).
  26. Citrin, P. H., *J. Amer. Chem. Soc.* **95**, 6472 (1973).
  27. Brant, P., and Stephenson, T. A., *Inorg. Chem.* **26**, 22 (1987).
  28. Lane, B. C., Lester, J. E., and Basolo, F., *J. Chem. Soc. Chem. Commun.*, 1618 (1971).
  29. Abruña, H. D., Meyer, T. J., and Murray, R. W., *Inorg. Chem.* **18**, 3233 (1979).
  30. Shpiro, E. S., Antoshin, G. V., Tkachenko, O. P., Gudkov, S. V., Romanovsky, B. V., and Minachev, Kh. M., in "Structure and Reactivity of Modified Zeolites" (P. A. Jacobs, N. I. Jaeger, P. Jiru, G. Schulzckloff, and V. B. Kazansky, Eds.), in "Studies in Surface Science and Catalysis," Vol. 18, pp. 31-39. Elsevier, Amsterdam, 1984.
  31. Citrin, P. H., and Ginsberg, A. P., *J. Amer. Chem. Soc.* **103**, 3673 (1981).
  32. Defosse, C., and Canesson, P., *React. Kinet. Catal. Lett.* **3**, 161 (1975).
  33. Canesson, P., Cruz, M. I., and Van Damme, H., in "International Clay Conference 1978" (M. M. Mortland, and V. C. Farmer, Eds.), in International Clay Conference 1978" (M. M. Mortland, and V. C. Farmer, Eds.), in "Developments in Sedimentology No. 27," pp. 217-225. Elsevier, Amsterdam, 1979.
  34. Noller, H., and Kladning, K., *Catal. Rev. Sci. Eng.* **13**, 194 (1976).
  35. Davis, B. H., Russell, S. N., Reucroft, P. J., and Shalvoy, R. B., *J. Chem. Soc. Faraday Trans. 1* **76**, 1917 (1980).
  36. La Ginestra, A., Patrono, P., Berardelli, M. L., Galli, P., Ferragina, C., and Massucci, M. A., *J. Catal.* **103**, 346 (1987).
  37. Segawa, K., Kurusu, Y., Nakajima, Y., and Kinoshita, M., *J. Catal.* **94**, 491 (1985).